Environment Protection Engineering

Vol. 49 2023 No. 3

DOI: 10.37190/epe230302

YAN CHEN[1], SHENGYUAN ZHU[1], WEI FANG[1]
HE HUANG[1], HAO QIN[2], SHENGTAO HU[2], YUZHAO WU[2]

EFFECTIVENESS OF FLY ASH ON THE STABILIZATION/SOLIDIFICATION OF Zn-CONTAMINATED SOIL

As a solid waste, the associated disposal cost of fly ash is really high. Previous studies suggested that the utilization of fly ash to treat heavy metal-contaminated soils was a new cost-effective method of disposal of it. Therefore, the effectiveness of fly ash stabilized/solidified Zn-contaminated soils has been investigated by unconfined compressive strength (UCS) and toxicity characteristics leaching procedure (TCLP) tests. Quantitative analysis of the soil microstructure was conducted by processing the X-ray diffraction (XRD) and scanning electron microscope (SEM) images. Mercury intrusion porosimetry (MIP) was carried out to illustrate the size and proportion of pore size for specimens under different ratios. The results of the tests showed an improvement in the UCS, which further increased as the content of binders was raised. Binder content would have little influence on the development of strength if the binder content exceeds a threshold value. The leached Zn^{2+} concentration of stabilized specimens was significantly decreased compared to that of untreated. Quantitative analysis confirmed that the addition of the binders resulted in the amount of hydration product, reduction of porosity, and a really random pores orientation, which was responsible for the improvement of the strength and leaching properties of the Zn^{2+} contaminated soils.

1. INTRODUCTION

Fly ash is a primary by-product of coal combustion during thermal power generation. Apart from the occupation of land resources, the inappropriate disposition of fly ash is likely to cause environmental pollution due to its toxicity and radioactivity [1, 2]. Around 221 million tons of fly ash are produced each year in the world, of which only

[1]China Jikan Research Institute of Engineering Investigations and Design Co., Ltd., No. 51, Xianning Middle Road, Xi'an, 710043, China.

[2]School of Resource and Environmental Engineering, Hefei University of Technology, Tunxi Road 193#, Baohe District, Hefei, 230009, China, corresponding author H. Qin, email address: geoqh@mail.hfut.edu.cn

around 60% is utilized, with the rest being dumped in ash ponds [3]. Despite the comprehensive utilization rate of fly ash has reached 70%, the stockpile of fly ash still remains at a very substantial tonnage [4].

Fly ash is a rich source of SiO_2 and Al_2O_3, as well as a little CaO, which makes fly ash a potential material in engineering construction activities such as producing cement and concrete, grouting, and sub-grade stabilization [5, 6]. Recently, some researchers turned attention to the potential of fly ash to treat problematic soils, alone or blended with other additives, owing to its self-cementing and pozzolanic properties as well as absorptivity [7]. It is confirmed that the engineering properties of soils can be successfully improved by treating fly ash [8]. Liu et al. [9] observed that tricalcium aluminate ($Ca_3Al_2O_6$) played a major role in the short-term strength, while the formation of gismondine ($CaAl_2Si_2O_8{\cdot}4H_2O$) and calcium silicate hydrates (CSHs) facilitated the long-term strength of the fly ash-lime stabilized specimens. Furthermore, it's worth noting that more and more research was performed to study the feasibility of fly ash in the remediation of heavy metal-contaminated soils [10].

Given that soil heavy metal pollution is increasingly serious and a large amount of fly ash is derived from thermal power plants annually, treating heavy metal-contaminated soils with fly ash may be a more cost-effective method to dispose of both heavy metal-contaminated soils and fly ash. Depending on the combined SiO_2, Al_2O_3, and Fe_2O_3 content, fly ash can be classified as class C and F. Previous studies indicated that class C fly ash has both self-cementing and pozzolanic properties, while class F fly ash just has pozzolanic properties [11]. In order to motivate the pozzolanic reactivity of fly ash optimally, its utilization was commonly accompanied by other alkaline additives [12]. While the availability of fly ash-stabilized heavy metal-contaminated soils alone has been rarely investigated.

Among the existing heavy metal-contaminated sites, Zn^{2+} is one of the most common heavy metal irons. Due to its extensive contamination and toxicity, Zn^{2+} is a serious risk to human health that has gained widespread attention [13]. This paper intends to evaluate the effectiveness of stabilized/solidified Zn-contaminated soils with class C fly ash (FA(C)) and class F fly ash (FA(F)). This assessment was carried out depending on the unconfined compressive strength (UCS) test and toxicity characteristic leaching procedure (TCLP) test. X-ray diffraction (XRD) and scanning electron microscope (SEM) technology were used to reveal the immobilized mechanism quantitatively by binarization processing. Finally, mercury intrusion porosimetry (MIP) was also carried out to illustrate the size and proportion of pore size for specimens under different ratios.

2. MATERIALS AND METHODS

Soil sample. The soil was sampled from a foundation pit in Hefei, China. The excavation depth was 4–5 m, and appeared yellowish-brown. Basic physical properties are pre-

sented in Table 1. The liquid limit of the tested soil was 49.4% and the plastic index was 24.6, respectively. Thus, the tested soil can be classified as low-liquid limit clay (CL) according to the Unified Soil Classification System [14].

Table 1

Basic physical properties of the tested soil

Density [g/cm^3]	Water content [%]	Gravity	Liquid limit [%]	Plastic limit [%]	Plastic index	Optimum water content [%]	Maximum density [g/cm^3]
1.92	25.5	2.669	49.4	24.8	24.6	21.2	1.663

Binders. Class C fly ash (FA(C)) and class F fly ash (FA(F)) were collected from the Hefei Union thermal power plant and Huaneng Chaohu power plant in China. Commercial Portland blast furnace slag cement (P325) was also prepared in order to indirectly evaluate the capacity of fly ash to stabilize heavy metal-contaminated soils. The main components of the two types of fly ash and cement were CaO, SiO_2, Al_2O_3, and Fe_2O_3 determined by using an X-ray fluorescence spectrometer (XRF-1800, Shimadzu, Japan), as shown in Table 2.

Table 2

Contents of main components of the soil, cement, and fly ash [%]

Composite	CaO	SiO_2	Al_2O_3	SO_3	Fe_2O_3	MgO	TiO_2	Na_2O
Soil	0.48	54.63	21.56	/	17.19	1.77	/	0.65
Cement	43.8	27.2	9.9	3.0	2.9	1.6	0.5	0.4
Fly ash (C)	31.52	38.72	14.48	2.16	7.21	4.49	/	0.77
Fly ash (F)	3.06	48.79	25.81	2.47	13.33	0.73	2.01	0.53

The contents of class C fly ash and cement were designed as 5, 10, and 15% at a mass ratio to dry soil (denoted as FA(C)5, FA(C)10 and FA(C)15; C5, C10, and C15, respectively). The content of class F fly ash was 10, 20, and 30% due to its low self-cementing properties (denoted as FA(F)10, FA(F)20 and FA(F)30, respectively).

Preparation of Zn-contaminated soil. Zn-contaminated soils belong to the most widely distributed heavy metal-contaminated soils in China. $Zn(NO_3)_2{\cdot}6H_2O$ was selected as the resource of the contaminants to artificially prepare Zn-contaminated soil due to their high solubility and low interference with the hydration process. Referring to the study of stabilization/solidification of Zn-contaminated soils by Liang et al. [13] and Liu et al. [15], the concentration was designed as 1000 and 5000 mg/kg at a mass ratio to dry soil (denoted as Zn0.1 and Zn0.5, respectively).

Sample preparation. Oven-dried soils and binders were initially pulverized and sieved with 2 mm and 0.5 mm sieves, respectively. Zn^{2+} solution was prepared by dissolving

$Zn(NO_3)_2 \cdot 6H_2O$ in distilled water. The soil was thoroughly mixed with $Zn(NO_3)_2$ solution, ensuring a complete and uniform interaction between Zn^{2+} ions and the soil samples. Subsequently, the mixture was stored in a curing room with a controlled humidity of 95±5% at 20 °C for 7 days. Then Zn-contaminated soil was oven-dried, pulverized, and again passed through a 2 mm sieve. Following this, a predetermined quantity of binders was added to the dried Zn-contaminated soils. Subsequently, a certain quantity of distilled water based on the optimum water content was poured into the mixture and stirred evenly. Cylindrical specimens (∅5 cm, *H* 5 cm) were prepared by a static compaction method depending on the 95% maximum dry density, which is listed in Table 1. Finally, the specimens were wrapped with plastic bags and stored in the standard curing room until tested at 28 days.

Unconfined compressive strength test was conducted on the specimens based on the ASTM Standard D5102 [16]. The test was performed at a loading rate of 0.4 mm/min. For each test, three parallel samples were set up and the data with a 10% error was considered valid.

Toxicity characteristic leaching test (USEPA Test Method TCLP 1311) was performed to evaluate the stability of Zn^{2+} ions immobilized in the specimens. Diluted acetic acid (5.7 cm^3 of acetic acid diluted with distilled water to 1000 cm^3) was used as a leachant (pH = 2.88±0.05). The specimens after the unconfined compression strength test were pulverized to pass through a 2 mm sieve. Delivered pellets were mixed with the leaching solution in a polypropylene bottle at a mass ratio of 1:20. The bottles were horizontally vibrated at 80 rpm in a water-bathing vibrator at 25 °C for 18 h. At the end of the extraction, the liquid was separated from the solids by filtration through a 0.45μm glass fiber filter. pH value was measured with a pH meter (PC60-Z, LABSEN, China), leached Zn^{2+} contents with an ICP-MS (Neptune Plus, Thermo Fisher, USA).

X-ray diffraction. The specimens were oven-dried at 105 °C for 24 h, pulverized, and passed through a 0.075 mm sieve. Then, X-ray diffraction (XRD) test was performed with Cu Kα radiation using a Rigaku D/Max-2005V diffractometer.

Scanning electron microscopy (SEM) test. To analyze the microstructure, the specimens, were freezing-dried and broken into small pieces ca. 5×5×5 mm. Then the samples were treated with a vacuum supply and metal spraying. In order to better reflect the information on soil particle arrangement and soil pores distribution, the SEM image was magnified 1000 times. Finally, the images were processed by binarization to extract the microstructure parameters, which can quantitatively describe the microstructure better. Tested specimens were divided into two parts: soil agglomerates and pores. To conduct the analysis, the SEM image was first converted into a binary image, where values of 0 (white pixel) and 1 (black pixel) corresponded to soil agglomerates and pores, respectively. Pixels with a grey value less than or equal to a predetermined threshold were

identified as pores, while those with a higher grey value were identified as soil agglomerates. In this study, MATLAB software was utilized for binarizing the SEM images and obtaining statistical pore results, with a threshold setting of 40.

Mercury intrusion porosimetry. The specimens were cut into small cubic pieces of approximately 3×3×3 mm, immediately immersed in liquid nitrogen, and freeze-dried in an Alpha 1-4 LDplus freeze-dryer for 24 h. A Quantachrome pore size meter (Auto-Pore IV 9500 V1.09, USA) was used to extract the specimens for mercury intrusion porosimetry (MIP) testing.

3. RESULTS AND DISCUSSION

3.1. UNCONFINED COMPRESSIVE STRENGTH

The results of unconfined compressive strength (UCS) of Zn-contaminated soils treated by various binders determined at 28-day curing time are shown in Fig. 1. Strength of the specimens was obviously improved by mixing the binders and increased with the increasing of binder content. UCS of cement-stabilized specimens was 3 times class C fly ash, and the strength of class C fly ash treated specimens was 2 times that of class F fly ash. Otherwise, although the superiority of the specimens stabilized with cement can be apparently observed, the UCS of specimens treated by fly ash still meet the regulatory limit of stabilized/solidified waste (0.34 MPa) [17].

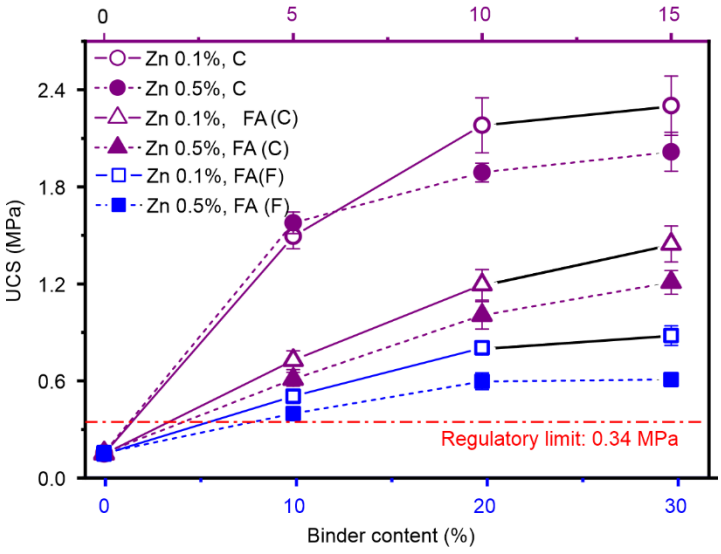

Fig. 1. Dependences of UCS for the Zn-contaminated soils stabilized with various binders on binders contents

The dependences of the growth rate of UCS (GR_{UCS}) of the stabilized Zn-contaminated soils on the binders content are presented in Fig. 2. The GR_{UCS} is defined as an increment of UCS with increasing binders content

$$GR_{UCS} = \frac{U_i - U_j}{i - j} \times 100\% \quad (1)$$

where U_i and U_j are UCSs of specimens stabilized by binders with different contents, MPa, i and j are binders contents, %, $j > i$.

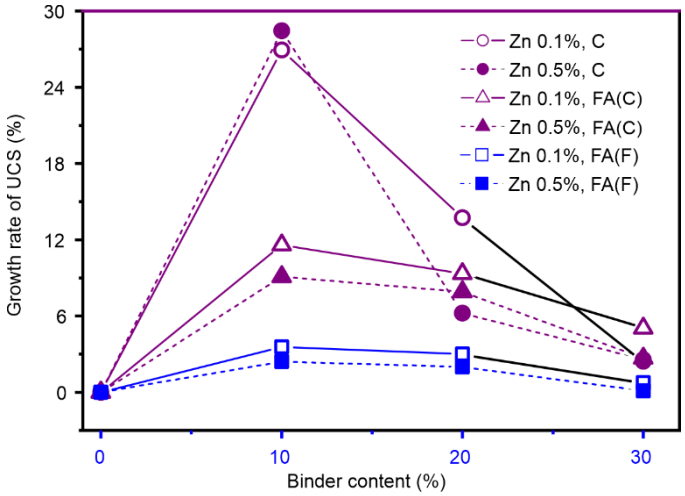

Fig. 2. Dependences of the growth rate of UCS (GR_{UCS}) of the stabilized Zn-contaminated soils on the binder content

As shown in Fig. 2, specimens stabilized with 5% cement and 5% class C fly ash, 10% class F fly ash obtained the maximum GR_{UCS}. Then the growth rate significantly linearly decreased with cement content increasing. While for the specimens treated with fly ash, the growth rate of UCS decreased slightly resulting from the increased binder content. It seems that the development of strength of cement-treated samples will diminish as the binder content exceeds a threshold value, and that of fly ash samples becomes constant.

For cement and fly ash stabilization, a significant increase in soil strength can be attributed to the formation of hydration products such as calcium silicate hydrate (CSH) and calcium aluminate hydrate (CAH) through hydration and pozzolanic reactions [18]. Cement stabilization resulted in an increase in strength due to the rapid reaction of tricalcium silicate (C_3S), dicalcium silicate (C_2S), tricalcium aluminate (C_3A), and dicalcium aluminate (C_2A) with water, leading to the activation of SiO_2 and Al_2O_3 in soil samples and the formation of CSH and CAH. In contrast, fly ash stabilization resulted in lower

strength, with the main mechanisms being pozzolanic reactions involving CaO, SiO_2, Al_2O_3, and H_2O. As shown in Table 2, the CaO content of class C and F fly ash were 31.52 and 3.06%, respectively. The limited amount of CaO in class F fly ash restricted the formation of pozzolanic reaction products, resulting in the lowest strength among the fly ash-stabilized specimens.

Besides, the UCS of the stabilized specimens with a higher concentration of Zn^{2+} was lower than that with a lower concentration, and the GR_{UCS} was a little slower. Increasing Zn^{2+} concentration hindered the development of UCS. Previous studies suggested that precipitates such $Zn(OH)_2$ and $Zn_2Ca(OH)_6{\cdot}2H_2O$ may have a detrimental influence on the development of hydrated reactions when the stabilized soils contained a little high concentration of Zn^{2+} [19].

3.2. LEACHING PROPERTIES

Figure 3 shows the variations of the leached Zn^{2+} concentration of the specimens stabilized with various binders. As shown in Fig. 3, the addition of binders can effectively decrease the Zn^{2+} leachability, and increasing binders content resulted in an obvious reduction of the leached Zn^{2+} concentrations. In a lower Zn^{2+} condition, the leached Zn^{2+} concentrations of all the specimens stabilized with the three types of binders satisfied the acceptance criteria (10 mg/dm^3 in the regulatory waste disposal limit at a disposal site of UK) except for the FA(F)10 stabilized specimens. Although fly ash failed to decrease the Zn^{2+} leachability to an acceptable value at a high Zn^{2+} concentration condition, the leached Zn^{2+} concentration was significantly decreased compared to that of untreated. It is concluded that fly ash can be a potential material to immobilize heavy metal ions.

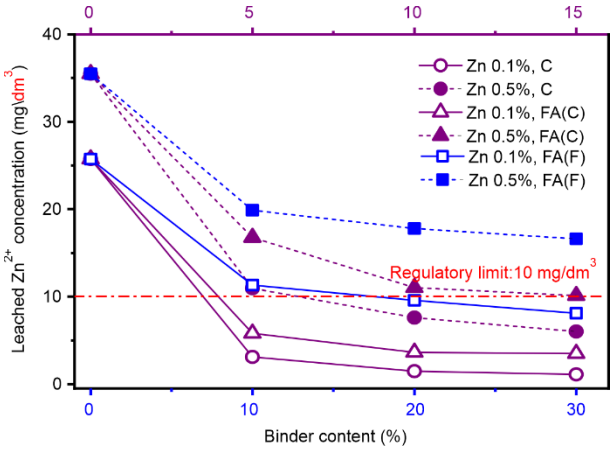

Fig. 3. Dependences of the leached Zn^{2+} concentration of the specimens stabilized with binders on the binder content

For the untreated contaminated soils, most of the Zn^{2+} dissociated in the pore solutions and adsorbed onto the surface of soil particles, which are susceptible to acidic conditions and released by desorption. In cement-stabilized soils, Zn^{2+} can be immobilized by precipitating as $Zn(OH)_2$ and adsorbed on the surface of hydrated Al oxide [20]. High alkaline conditions offered by the cement hydration may convert $Zn(OH)_2$ into $Zn(OH)_4^{2-}$ or $Zn(OH)_5^{3-}$ which can interact with Ca^{2+} to form $CaZn_2(OH)_6{\cdot}H_2O$. Zn^{2+} ions can substitute for Ca^{2+} ones in CSH, and immobilize by chemical incorporation [21]. Therefore, Zn^{2+} leachability can be effectively decreased by cement treatment. For fly ash-treated soils, besides precipitation, encapsulation, and substitution, adsorption may be the predominant mechanism of Zn^{2+} immobilization. In addition, the leaching concentration of FA(C) is lower than that of FA(F) for the same Zn^{2+} concentration of contaminated soil (Fig. 3). The reason is the difference in the CaO content of C and F fly ash, where the amount of CaO determines the amount of pozzolanic reaction products. The sorption of Zn^{2+} by hydrated gels makes the difference [22].

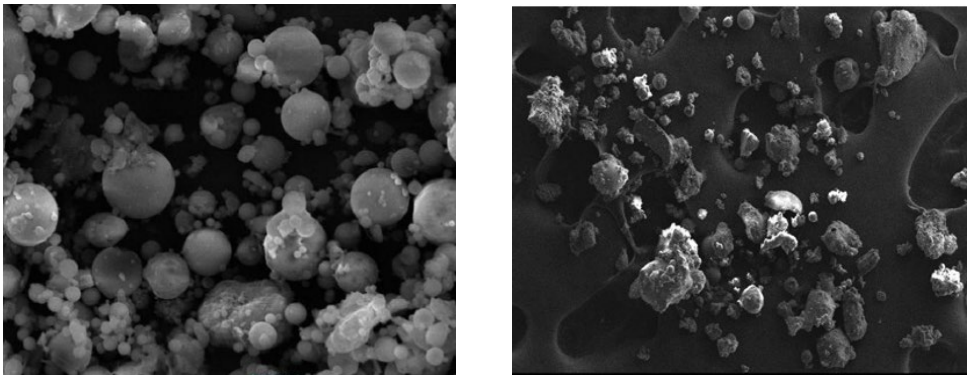

Fig. 4. Microstructure characteristics of fly ash:
a) image of fly ash, b) morphology of cenosphere [5, 23]

As shown in Fig. 4, fly ash was composed of a large quantity of cenosphere, and these hollow spheres were characterized as porous media, leading to a high specific surface area. Thus, Zn^{2+} ions can be successfully adsorbed onto the surface of the cenosphere. Besides, the non-burned carbon in the fly ash can also adsorb Zn^{2+} sufficiently for its high specific surface area [24].

3.3. QUANTITATIVE ANALYSIS BASED ON MICROSTRUCTURE

XRD patterns of the specimens stabilized with various binders are shown in Fig. 5. The hydration gels of CSH, and CAH are mainly produced, and the ettringite (AFt), calcium hydroxide (CH), and calcium monosulfoaluminate hydrate (AFm) is additionally formed. Hydration product generation confirms the pozzolanic properties of fly ash

and cement, which causes significant improvement in UCS as shown in Figs. 1 and 2. Results for soils stabilized with different classes of fly ash are shown in Fig. 5, curves b and c. With hydration products in both FA(F) and FA(C), the amount of hydration products increases with the accelerated pozzolanic reactions, which confirms the component supplementary caused by calcite-enriched binders incorporation. The differences between FA(F) and FA(C) in the UCS and leaching characteristics are verified in Figs. 1–3.

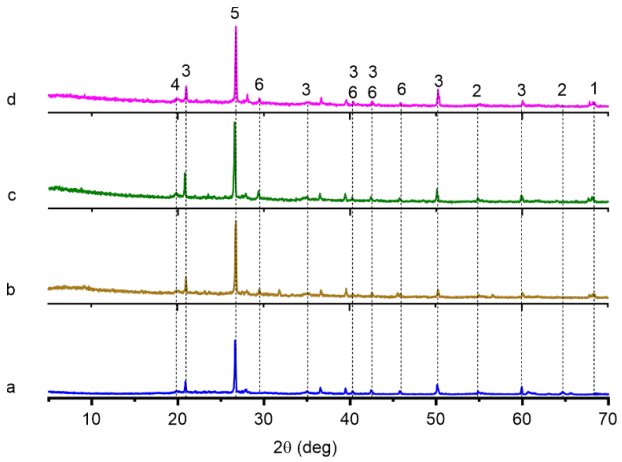

Fig. 5. XRD patterns of the specimens stabilized with binders: a) without binders, b) FA(F)30, c) FA(C)15, d) C10; 1 – CAH, 2 – CH, 3 – AFb, 4 – AFm, 5 – quartz, 6 – CSH

Figure 6 shows the SEM images of the untreated and stabilized samples (contaminated with 1000 mg/kg of Zn^{2+}) before and after binarization. In order to describe the microstructure quantitatively, the porosity and pore orientation of the specimens were extracted from the binarized images.

As shown in Fig. 7, the porosity decreased after stabilizing with binders. C10 stabilized specimens exhibited the maximum reduction rate of porosity, and that of FA(F)30 was the lowest. That was corresponding to the variations of UCS after stabilization. Some products of hydration and pozzolanic reaction filled the soil pores, leading to a denser structure and enhancing the soil strength.

In Figure 8, the distribution of soil pore orientation in stabilized samples with respect to untreated samples has been shown. The untreated soil exhibits a high degree of pore directionality, with the majority of pores oriented in the same direction and relatively low anisotropy (Fig. 8a). The addition of cement and fly ash resulted in a more random distribution of pore orientation. Lime-stabilized specimens show a predominance of vertically and horizontally oriented pores, class C fly ash exhibits predominantly vertical pore orientation, and class F fly ash shows a more discrete and random orientation (Figs. 8b–d).

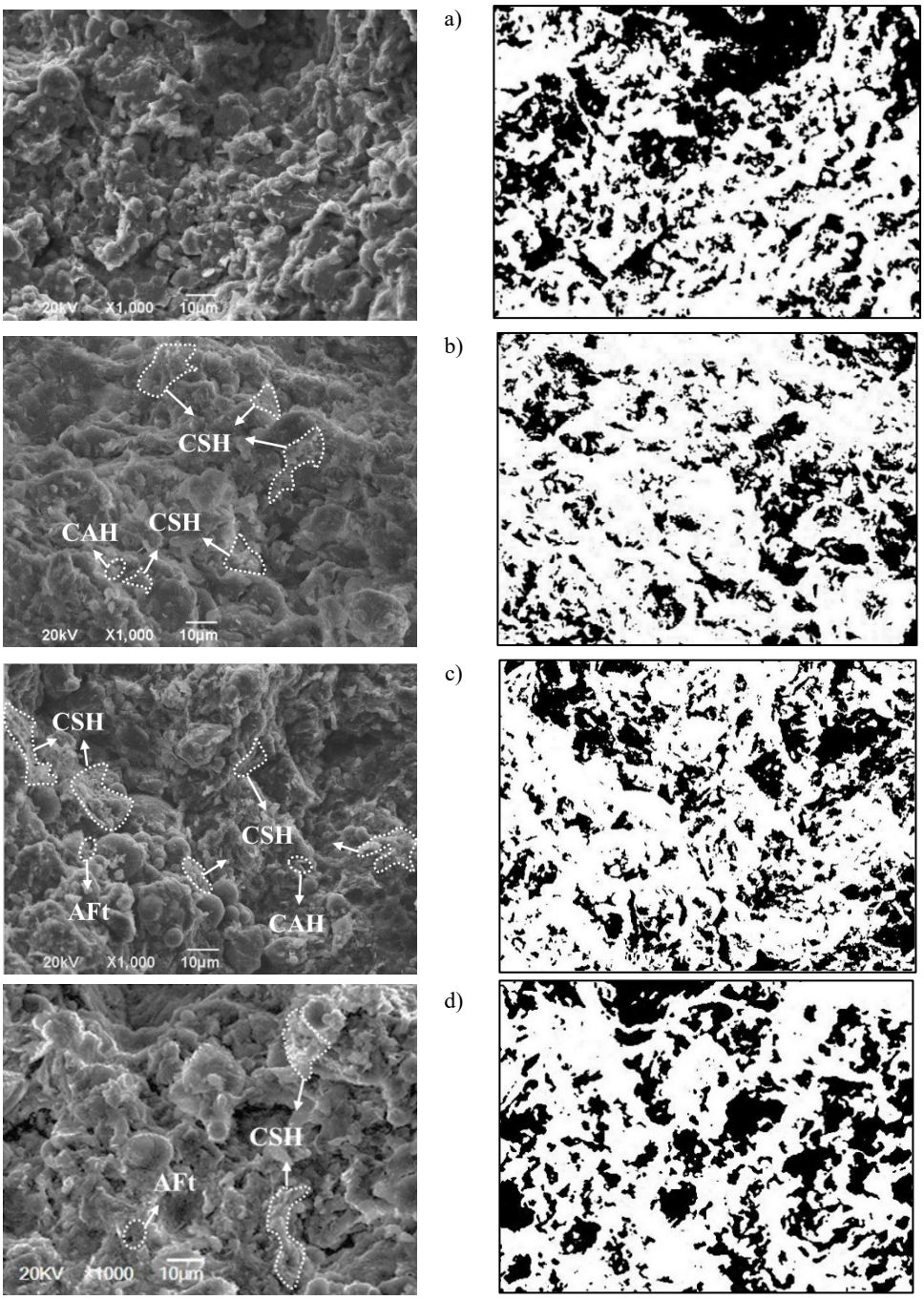

Fig. 6. SEM images(left) and binary images (right) of the specimens stabilized with different binders: a) without binders, b) stabilized with C10, c) stabilized with FA(C)15, d) stabilized with FA(F)30

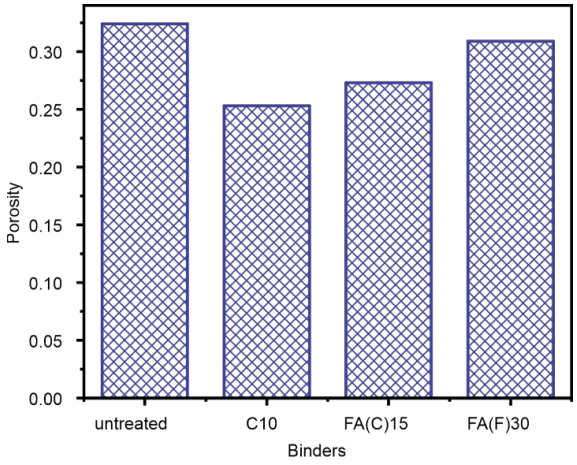

Fig. 7. Porosity of the specimens after stabilization with various binders

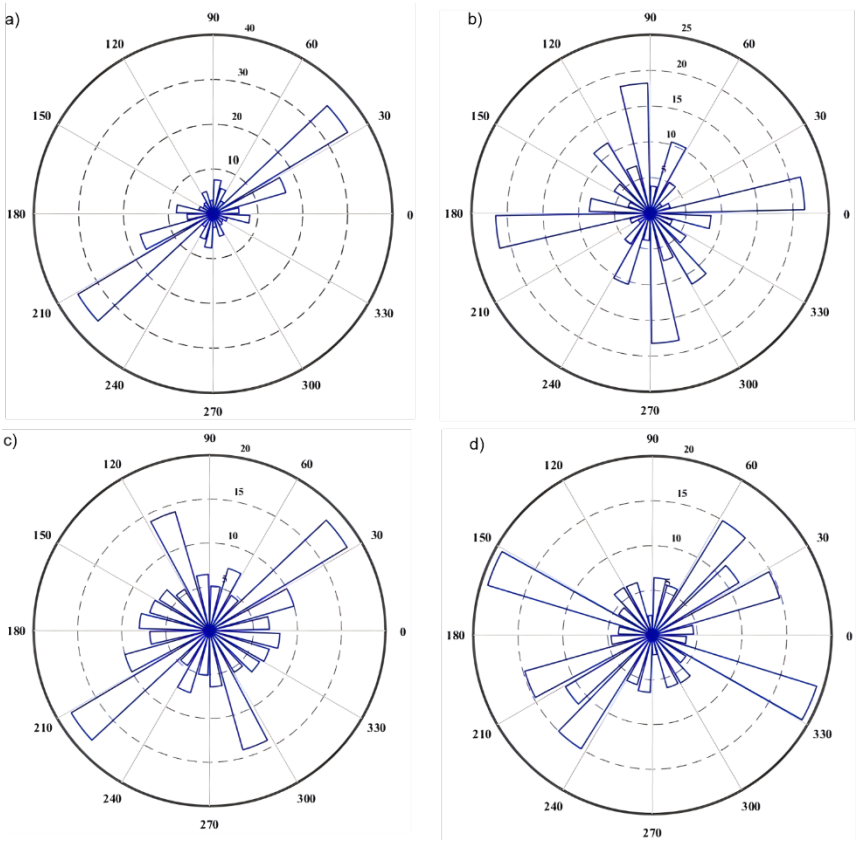

Fig. 8. Soil pores orientation of the specimens stabilized with various binders

These results suggest that the addition of binders altered the pore structure of the soils, which in turn led to improvements in soil strength and reduced leachability of Zn^{2+}. The quantity of hydration products produced by the binders may play a significant role in determining pore directionality, with higher amounts resulting in more pronounced directionality and lower amounts leading to a more random distribution of pore orientation.

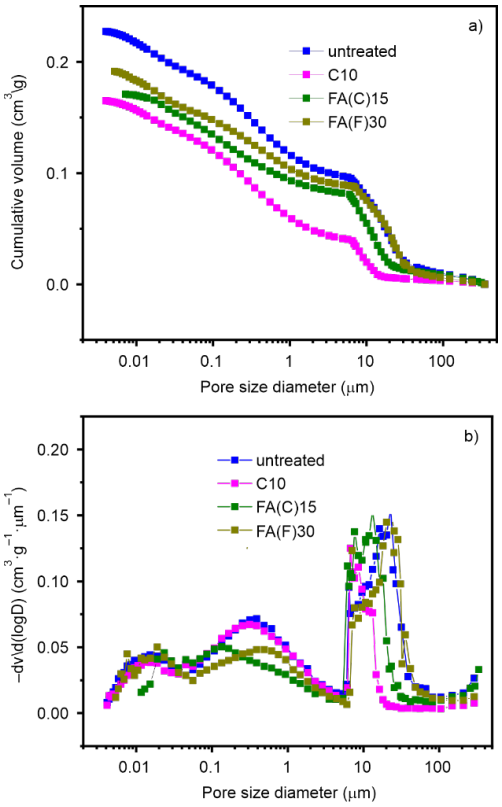

Fig. 9. Results of mercury intrusion porosimetry (MIP) tests of the specimens stabilized with various binders

Figure 9 shows the variation in pore size following the stabilization of the specimens. The addition of binders results in a significant reduction in the total pore volume of the specimens (Fig. 9a). The C10 specimen has the lowest total pore volume, followed by FA(C)15, while FA(F)30 has the largest total pore volume, although still lower than that of the untreated specimen. Figure 9b exhibits a double-peak structure, with the first peak of the untreated specimen (corresponding to a diameter of 0.3–0.4 μm) remaining relatively unchanged after the addition of cement. However, the peak shifted slightly to the left and right with the addition of C and F class fly ash, respectively,

suggesting a reduction in pore volume in the 0.3–0.4 μm diameter range with C class fly ash, and an increase with F class fly ash. The second peak of the untreated specimen (corresponding to a diameter of 20–30 μm) moves significantly to the left following the addition of cement and class C fly ash, indicating a reduction in pore volume due to hydration products from the pozzolanic reaction. Conversely, the peak shows a lack of movement after the addition of class F fly ash, indicating a lower efficacy of hydration products in reducing pore space in the specimens.

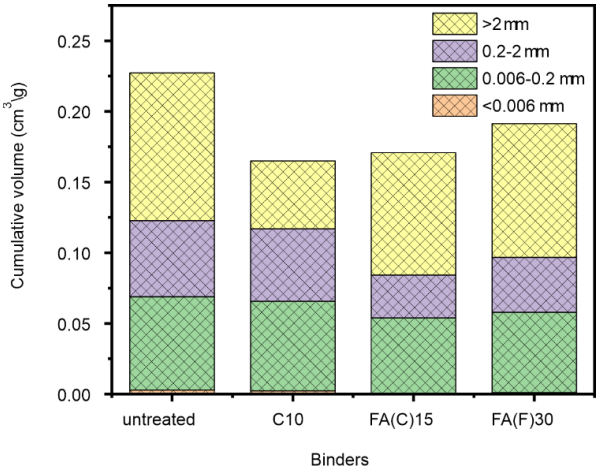

Fig. 10. Pore size proportions of the specimens after stabilization with various binders

As shown in Fig. 10, the pores present may be divided into large (>2 μm), small (0.2–2 μm), micro (0.006–0.2 μm), and undetectable pores (<0.006 μm) [25]. With the addition of a binder, the total specimen pore volume is reduced, however, different binders lead to changes in the proportion of different pores. Following the cement addition, an increased proportion of small and micropores and a decreased proportion of large pores are observed in the specimens. In contrast, the addition of fly ash increased the proportion of large and micropores, decreasing the proportion of small pores. Specimen with class C fly ash had a higher proportion of large pores and micropores than the specimen stabilized with class F fly ash. It is clear that the fly ash stabilized specimens mainly by reducing the proportion of small pores and enhancing the proportion of micro- and macropores.

4. CONCLUSIONS

After stabilization, the UCS of the specimens can be enhanced significantly and increased with binder content increase. Cement-stabilized specimens got a really high

UCS that was 3 times class C fly ash. The strength of class C fly ash treated specimens was 2 times that of class F fly ash.

Increasing binder content would have little influence on the development of strength if the binder content exceeds a threshold value.

The leached Zn^{2+} concentration of stabilized specimens was significantly decreased compared to that of untreated, although fly ash failed to decrease the Zn^{2+} leachability to an acceptable value at a high Zn^{2+} concentration condition.

Quantitative analysis based on the XRD patterns, binarized SEM images, and MIP results confirmed that the addition of the binders resulted in the amount of hydration products, reduction of porosity, and a really random pores orientation, which is responsible for the improvement of the strength and leaching properties of the Zn^{2+} contaminated soils.

Based on the results of UCS and TCLP, class C and F fly ash were proved to be potential materials to treat contaminated soils with a low concentration.

ACKNOWLEDGMENT

The research has been financed by the Anhui Soft Science Research Program Project (202106f01050006).

REFERENCES

[1] BAEK J.W., CHOI A.E.S., PARK H.S., *Solidification/stabilization of ASR fly ash using Thiomer material: Optimization of compressive strength and heavy metals leaching*, Waste. Manage., 2017, 70, 139–148. DOI: 10.1016/j.wasman.2017.09.010.

[2] KAZAKIS N., KANTIRANIS N., KALAITZIDOU K., KAPRARA E., MITRAKAS M., FREI R., VARGEMEZIS G., VOGIATZIS D., ZOUBOULIS A., FILIPPIDIS A., *Environmentally available hexavalent chromium in soils and sediments impacted by dispersed fly ash in Sarigkiol basin (Northern Greece)*, Environ. Pollut., 2018, 235, 632–641. DOI: 10.1016/j.envpol.2017.12.117.

[3] GADORE V., AHMARUZZAMAN M., *Tailored fly ash materials: A recent progress of their properties and applications for remediation of organic and inorganic contaminants from water*, J. Water. Proc. Eng., 2021, 41, 101910. DOI: 10.1016/j.jwpe.2020.101910.

[4] WANG C., XU G.G., GU X.Y., GAO Y.H., ZHAO P., *High value-added applications of coal fly ash in the form of porous materials: a review*, Ceram. Int., 2021, 47 (16), 22302–22315. DOI: 10.1016/j.ceramint.2021.05.070.

[5] NGUYEN T.B.T., CHATCHAWAN R., SAENGSOY W., TANGTERMSIRIKUL S., SUGIYAMA T., *Influences of different types of fly ash and confinement on performances of expansive mortars and concretes*, Constr. Build. Mater., 2019, 209, 176–186. DOI: 10.1016/j.conbuildmat.2019.03.032.

[6] BROCHOCKA A., NOWAK A., PANEK R., KOZIKOWSKI P., FRANU W., *Effective removal of odors from air with polymer nonwoven structures doped by porous materials to use in respiratory protective devices*, Arch. Environ. Prot., 2021, 47 (2), 3–19. DOI: 10.24425/aep.2021.137274.

[7] JHA A.K., SIVAPULLAIAH P.V., *Physical and strength development in lime treated gypseous soil with fly ash. Micro-analyses*, Appl. Clay Sci., 2017, 145, 17–27. DOI: 10.1016/j.clay.2017.05.016.

[8] XIAO H.W., WANG W., GOH S.H., *Effectiveness study for fly ash cement improved marine clay*, Constr. Build. Mater., 2017, 157, 1053–1064. DOI: 10.1016/j.conbuildmat.2017.09.070.

[9] LIU S.T., LI Z.Z., LI Y.Y., CAO W.D., *Strength properties of Bayer red mud stabilized by lime-fly ash using orthogonal experiments*, Constr. Build. Mater., 2018, 166, 554–563. DOI: 10.1016/j.conbuildmat.2018.01.186.
[10] DERMATAS D., MENG X.G., *Utilization of fly ash for stabilization/solidification of heavy metal-contaminated soils*, Eng. Geol., 2003, 70, 377–394. DOI: 10.1016/S0013-7952 (03)00105-4.
[11] SONI R., *Behavior of fly ash in cement-concrete pavement*, Int. Res. J. Eng. Technol., 2015, 2, 368–372.
[12] PHUMMIPHANA I., HORPIBULSUKB S., RACHANC R., ARULRAJAHD A., SHENE S., CHINDAPRASIRTF P., *High calcium fly ash geopolymer stabilized lateritic soil and granulated blast furnace slag blends as a pavement base material*, J. Hazard. Mater., 2018, 341, 257–267. DOI: 10.1016/j.jhazmat.2021.125205.
[13] LIANG S.H., DAI J., NIU J.G., WANG M., WANG L.P., DONG J.H., *Solidification of additives for zinc-contaminated silt*, Adv. Mech. Eng., 2018, 10 (7), 1687814018789238. DOI: 10.1177/1687814018789238.
[14] ASTM Standard D2487, *Standard practice for classification of soils for engineering purposes (unified soil classification system)*, 2000. DOI: 10.1520/D2487-17E01.
[15] LIU J.J., ZHA F.S., XU L., KANG B., TAN X.H., DENG Y.F., YANG C.B., *Mechanism of stabilized/solidified heavy metal-contaminated soils with cement-fly ash based on electrical resistivity measurements*, Measure., 2019, 141, 85–94. DOI: 10.1016/j.measurement.2019.03.070.
[16] ASTM Standard D5102, *Standard Test Methods for Unconfined Compressive Strength of Compacted Soil-Lime Mixtures*, 2004. DOI: 10.1520/D5102_D5102M-22.
[17] SOLLARS C.J., PERRY R., *Cement-based stabilization of waste: practical and theoretical considerations*, Water Environ. J., 1989, 3 (2), 125–134. DOI: 10.1111/j.1747-6593.1989.tb01500.x.
[18] QIAO X.C., *Solidification and stabilization of heavy metal waste using reject fly ash activated by FGD*, Wu Han University of Technology, doctoral dissertation, Wu Han 2004.
[19] YOUSUF M., MOLLAH A., VEMPATI K., LIN T.C., COCKE D.L., *The interfacial chemistry of solidification/stabilization of metals in cement and pozzolanic materials systems*, Waste. Manage., 1995, 15, 137–148. DOI: 10.1016/0956-053X (95)00013-P.
[20] SHUMAN L.M., *Adsorption of Zn by Fe and Al hydrous oxides as influenced by aging and pH*, Soil. Sci. Soc. Am. J., 1977, 41 (4), 703–706. DOI: 10.2136/sssaj1977.03615995004100040016x.
[21] PANDEY B., KINRADE S.D., CATALAN L.J.J., *Effects of carbonation on the leachability and compressive strength of cement-solidified and geopolymer-solidified synthetic metal wastes*, J. Environ. Manage., 2012, 101, 59–67. DOI: 10.1016/j.jenvman.2012.01.029.
[22] SRIVASTAVA V.C., MALL I.D., MISHRA I.M., *Modelling individual and competitive adsorption of cadmium (II) and zinc (II) metal ions from aqueous solution onto bagasse fly ash*, Sep. Sci. Technol., 2006, 41, 2685–2710. DOI: 10.1080/01496390600725687.
[23] KUMARA K., KUMAR S., GUPTA M., GARG H.G., *Characteristics of fly ash in relation of soil amendment*, Materials Today: Proc., 2017, 4, 527–532. DOI: 10.1016/j.matpr.2017.01.053.
[24] AHMARUZZAMAN M., *A review on the utilization of fly ash*, Prog. Energ. Combust., 2010, 36, 327–363. DOI: 10.1016/j.pecs.2009.11.003.
[25] BIAN X., ZENG L.L., LI X.Z., SHI X.S., ZHOU S.M., LI F.Q., *Fabric changes induced by super-absorbent polymer on cement-lime stabilized excavated clayey soil*, J. Rock. Mech. Geotech., 2021, 13 (5), 1124–1135. DOI: 10.1016/j.jrmge.2021.03.006.